

# On-orbit performance of the Far Ultraviolet Spectroscopic Explorer (*FUSE*)

David J. Sahnou<sup>\*a</sup>, H. Warren Moos<sup>a</sup>, Thomas B. Ake<sup>a</sup>, B-G Andersson<sup>a</sup>, Martial Andre<sup>a,b</sup>, David Artis<sup>c</sup>, Alice F. Berman<sup>a</sup>, William P. Blair<sup>a</sup>, Kenneth R. Brownsberger<sup>d</sup>, Humberto M Calvani<sup>a</sup>, Pierre Chayer<sup>a,e</sup>, Steven J. Conard<sup>a</sup>, Paul D. Feldman<sup>a</sup>, Scott D. Friedman<sup>a</sup>, Alex W. Fullerton<sup>a,e</sup>, Geoffrey A. Gaines<sup>f</sup>, James C. Green<sup>d</sup>, Mark A. Gummin<sup>g</sup>, J. B. Joyce<sup>a</sup>, Mary Elizabeth Kaiser<sup>a</sup>, Jeffrey W. Kruk<sup>a</sup>, Don J. Lindler<sup>h</sup>, Derck Massa<sup>i</sup>, Edward M. Murphy<sup>a</sup>, William R. Oegerle<sup>a</sup>, Raymond G. Ohl<sup>a</sup>, Steven N. Osterman<sup>d</sup>, Bryce A. Roberts<sup>a</sup>, Katherine C. Roth<sup>a</sup>, Ravi Sankrit<sup>a</sup>, Kenneth R. Sembach<sup>a</sup>, Robin L. Shelton<sup>a</sup>, Oswald H. W. Siegmund<sup>f</sup>, Harold A. Weaver<sup>a</sup>, Erik Wilkinson<sup>d</sup>

<sup>a</sup> Center for Astrophysical Sciences, Department of Physics and Astronomy,  
The Johns Hopkins University, Charles & 34<sup>th</sup> Streets, Baltimore, MD 21218

<sup>b</sup> Institut d'Astrophysique de Paris, INSU CNRS, 98 bis Boulevard Arago, F-75014 Paris, France

<sup>c</sup> The Johns Hopkins University Applied Physics Laboratory, Laurel, MD 20723

<sup>d</sup> Center for Astrophysics & Space Astronomy, University of Colorado, Campus Box 593, Boulder, CO  
80309-0593

<sup>e</sup> Dept. of Physics & Astronomy, University of Victoria, P.O. Box 3055, Victoria, BC, V8W 3P6,  
Canada

<sup>f</sup> Space Sciences Laboratory, University of California, Berkeley, CA 94720-7450

<sup>g</sup> MAG Systems, 1731 Saint Andrews Ct., St. Helena, CA 94574

<sup>h</sup> Advanced Computer Concepts, Inc., Code 681, Goddard Space Flight Center, Greenbelt, MD 20771

<sup>i</sup> Raytheon ITSS, Code 681, Goddard Space Flight Center, Greenbelt, MD 20771

## ABSTRACT

The *Far Ultraviolet Spectroscopic Explorer* (FUSE) satellite was launched into orbit on June 24, 1999. FUSE is now making high resolution ( $\lambda/\Delta\lambda = 20,000 - 25,000$ ) observations of solar system, galactic, and extragalactic targets in the far ultraviolet wavelength region (905 - 1187 Å). Its high effective area, low background, and planned three year life allow observations of objects which have been too faint for previous high resolution instruments in this wavelength range.

In this paper, we describe the on-orbit performance of the *FUSE* satellite during its first nine months of operation, including measurements of sensitivity and resolution.

**Keywords:** Astronomy, ultraviolet, spectroscopy, Far Ultraviolet Spectroscopic Explorer, FUSE.

---

\*Correspondence: Email: sahnou@pha.jhu.edu; WWW: <http://fuse.pha.jhu.edu>; Telephone: 410 516 8503;  
Fax: 410 516 5494

## 1. INTRODUCTION

The *Far Ultraviolet Spectroscopic Explorer (FUSE)* was launched into a 768 km low earth orbit on June 24, 1999. After an initial period of on-orbit guidance tests, the two far ultraviolet detectors were powered on in August, 1999, and several months of In Orbit Checkout and Science Verification activities began. This included investigations of the instrument performance, and preliminary instrument characterization. Although a transition to normal science operations was made in late 1999, characterization activity will continue throughout the three year mission at a continually decreasing frequency. Results from these early investigations show that the satellite is generally performing well; most measures show that the performance is at or near preflight predictions. This paper will briefly describe the design of FUSE, and present the results of on-orbit performance tests, as of March, 2000.

*FUSE* was designed to obtain high resolution, far ultraviolet spectra of faint astronomical objects in the 905 - 1187 Å wavelength range. This mission, built as part of the NASA *Origins* program, will address many important astrophysical problems, including the measurement of the deuterium to hydrogen ratio, the distribution of hot gas in the Galaxy, and the properties of molecular hydrogen in interstellar clouds. *FUSE* is the first long-duration mission to obtain high resolution spectra in this wavelength region since *Copernicus* in the 1970s. Since that time, important advances have been made in mirror coating technology and in the development of large format detectors with low background. These and other improvements allow *FUSE* to make significant performance gains over *Copernicus*. An overview of the mission and its scientific objectives has been given by Moos et al.<sup>1</sup>

## 2. DESIGN AND IMPLEMENTATION

The FUSE instrument (**Figure 1**) consists of four coaligned optical channels. Each channel is made up of an off-axis parabolic primary mirror, a focal plane assembly (FPA) containing four spectrograph entrance apertures, a large, holographically-ruled, aberration-corrected spherical grating with a high groove density, and half of a double delay line microchannel plate detector. The gratings and mirrors of two of the channels are coated with silicon carbide (SiC), which provides an approximately constant reflectivity across the entire FUSE bandpass, while the remaining two are coated with lithium fluoride (LiF) over aluminum, in order to maximize the instrument throughput above ~1000 Å. This design limits the number of reflections in each channel to two, which is important in the ultraviolet where reflectivities are typically poor. In addition, the multiple channel design ensures that nearly the entire wavelength range is covered by multiple channels. This redundancy was included to ensure that a partial failure did not compromise the wavelength coverage, while simultaneously maximizing the effective area from ~1000 to 1100 Å, where all four channels overlap in wavelength coverage. Details of its design and the predicted performance based on preflight measurements have been given previously<sup>2,3</sup>.

The optical design is identical for the two LiF channels; the wavelength coverage differs only because the two detectors are slightly shifted with respect to each other along the Rowland circle. This offset allows gaps in the wavelength coverage due to spaces between the detector segments to fall at different wavelengths on the two channels. The two SiC channel designs are also identical. The SiC and LiF channels have slightly different dispersions (averaging 1.03 Å/mm and 1.12 Å/mm respectively). The optical design leads to different two dimensional point spread functions between the SiC and LiF channels<sup>4</sup>. The astigmatic heights of the spectra (and consequently the resolution) vary between ~200 μm and ~1200 μm across the FUSE spectral band. Also, because of differences in the alignment of identically-designed channels, the focus can be slightly

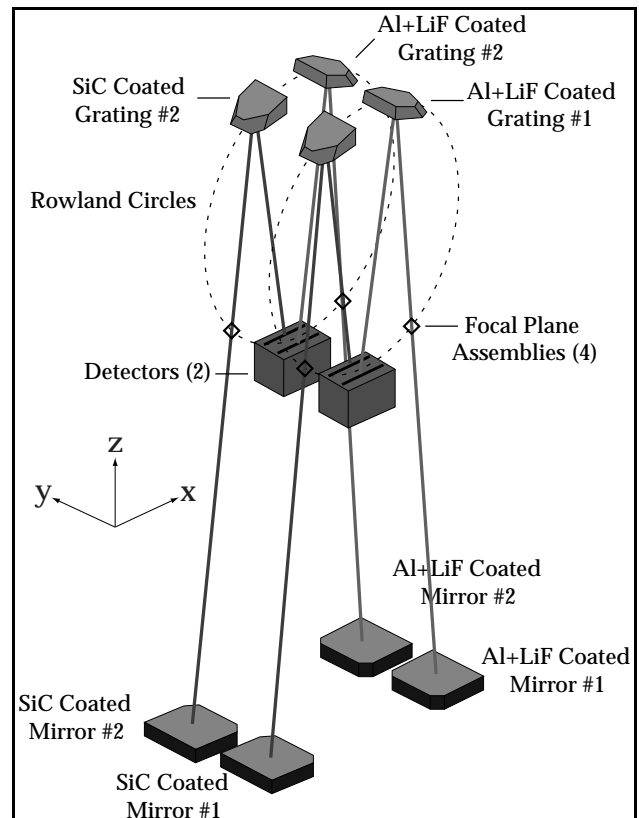


**Figure 1** A schematic view of the FUSE optical system.

different between channels, and the intrinsic resolution of the two detectors differs – which means that even two channels with identical designs can have substantially different resolving powers at the same wavelength.

The apertures in the FPAs include a narrow 1.25" × 20" slit (HIRS) for maximum resolution, an intermediate 4" × 20" (MDRS), and a large 30" × 30" (LWRS) for maximum throughput. The FPAs can be adjusted in the dispersion direction in order to coalign the four channels, and in the focus direction to maintain spectrograph focus. In addition, the telescope mirrors can be adjusted in focus, tip, and tilt in order to maintain coalignment and focus the mirrors to the FPAs; the gratings and detectors are fixed on orbit. The satellite pointing is adjusted in order to select a particular aperture once the channels are aligned using the mirrors and FPAs. A visible-light Fine Error Sensor (FES), which views the FPA on one of the LiF channels, is used to maintain pointing using stars within a 20' × 20' field around the target.

The two FUSE detectors are windowless, multi-segment, large format, two dimensional microchannel plate (MCP) detectors with helical double delay line (DDL) anodes. A detector consists of two segments, each with an active area of 88 × 10 mm; these segments are separated by a gap of < 10 mm. The front surface of each MCP is coated with a KBr photocathode in order to maximize the far ultraviolet response. Quantum efficiencies are in the range of 14 – 30% in the FUSE bandpass, depending on the segment and the wavelength range. On orbit, a mechanical door which protected the photocathode during ground testing and launch was opened once the spectrograph cavity pressure reached an acceptable level. Ion pumps were then used to monitor the pressure in the spectrograph cavity until it dropped low enough for high voltage operations to begin. High voltage operations of the two detectors began in mid to late August, 1999. Details of the design of the FUSE detectors has been given elsewhere<sup>5</sup>.

The size and location of pixels in DDL detectors are not fixed, but are determined by timing and analog measurements. The detector pixels are digitized to approximately 6 μm (~6 mÅ) in the dispersion direction, and 10 – 17 μm (depending on segment) in the cross dispersion direction, for a full extent of 16384 × 1024 pixels. The intrinsic detector resolution, however, due to the MCP pore size and spacing of 10 – 15 μm and the design of the electronics, is limited to ~20 μm × ~80 μm FWHM.

Data collected by the detectors is sent via the science data bus to the Instrument Data System (IDS). The IDS is responsible for storing this data as individual photon events (time tag or TTAG mode) with periodic time markers (typically once per second), or assembling the data into a two-dimensional histogram (spectral image or HIST mode). Targets with a total count rate less than ~2,000 cps are taken in time tag mode in order to preserve information on the arrival time of the photons. At higher count rates (up to ~32,000 cps), the onboard memory would be quickly exhausted, so the data from only the relevant part of the detector is binned (typically by 8) in the y direction and stored as a two-dimensional image. Since the arrival times of the individual photons are lost in this process, Doppler corrections for the orbital velocity can only be made on the image as a whole; as a result, each observation is divided into multiple exposures during each orbit. The y binning has a negligible effect on the resolution of the data.

The FUSE spacecraft bus, built by Orbital Sciences Corporation and located below the instrument section, consists of the power, attitude control, and communications systems for the satellite. The instrument and spacecraft together make up the FUSE satellite.

Operations are controlled from a Satellite Control Center (SCC) at the Johns Hopkins University. Operations are described in section 7.1.

### **3. DETECTOR PERFORMANCE**

#### **3.1. Flat Field and Signal to Noise**

An onboard mercury-vapor stimulation lamp permits a roughly uniform illumination of each detector. Because of count rate limitations of the detector electronics, however, it is not practical to take deep flat fields on orbit; in addition, grid wires from the detector's ion repeller and plasma grids shadow parts of the detector when illuminating the detector this way. Before launch, flat field images were taken with a diffuser in front of the detector in order to minimize the effect of the grid wires. These flat fields contain 40 – 100 events per pixel, which is sufficient to obtain a signal-to-noise ratio of 50 – 120 per a spectrograph resolution element of 6 pixels in the x direction and 7 – 70 pixels in the y dimension (depending on wavelength and channel). It had been expected that the much lower signal-to-noise stim lamp exposures could then be used to transform the ground based

flats into the flight reference frame, and to monitor any gross changes in response; however, recent measurements show that the changing thermal conditions during the time that the ground flats were taken will make this impossible. Instead, flat fields will be derived from in-flight measurements of bright white dwarfs.

**Figure 2** shows several regions of one of the ground flat field images for segment 1A. The ground-based flats show a complex structure containing dead spots due to blocked pores, brush marks from cleaning of the MCPs before assembly, multifiber bundle hex boundaries, and moiré features<sup>6</sup> due to a beating between MCPs. These same features appear, along with a stretch and shift due to changes in detector electronics temperature (to the limits of the S/N of the measurements) on orbit, which is consistent with previous missions using similar detectors. The fixed pattern noise, particularly the moiré with a periodicity of about 50  $\mu\text{m}$ , limits the ability to make very high signal to noise measurements without dithering, or moving the spectrum on the detector during an observation. The two dimensional detector format means that a given spectrum falls on

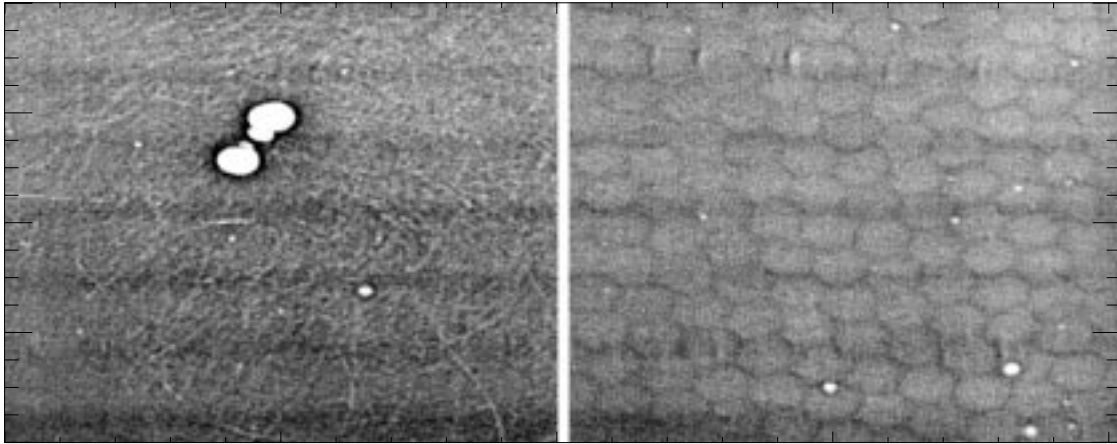


**Figure 2** A reversed image of two regions from the ground-based flat field on detector segment 1A, showing typical features. The image on the left shows several large dead spots with bright rims, along with brush marks. The image on the right shows the chicken wire pattern from the MCP hex boundaries. Shadows of the grids are seen as faint horizontal stripes.

millions of pixels. Since it is not possible to determine the flat field all of those pixels to high S/N, a simple shift and add, or averaging approach is being taken for observations where the highest signal-to-noise is required. This allows a given part of the spectrum to sample multiple regions on the detector and nearly recovers the S/N expected from Poisson statistics alone. Using this method, a signal-to-noise of 120 per spectral resolution element was demonstrated during the instrument checkout period.

### 3.2. Background

The apparent detector background, from a combination of residual radioactivity in the MCPs<sup>7</sup>, cosmic rays, other high energy particles, and scattered light, is approximately 0.8 counts/cm<sup>2</sup>/sec on all four segments; reasonable pulse height thresholds can reduce this number by a factor of two. Before launch, when the particle background was not present, typical rates were ~0.35 counts/cm<sup>2</sup>/sec. Because there is no shutter on the FUSE instrument, the detectors are constantly collecting photons, primarily from airglow when there is no target in the apertures. This contamination means it is not possible to get an accurate background measurement from the detectors in the region where the spectra fall. Thus, unused regions of the detector are used to measure this effect. Since there appears to be no identifiable structure to the background, no spatial variation has been assumed.

### 3.3. Single Event Upsets

The only significant detector anomaly discovered on orbit was the sensitivity of the electronics to single event upsets (SEUs). When the detector electronics were powered on after launch, the detector data processing unit began reporting errors in the memory which stores the code controlling the detector. Further investigation revealed that the memory was being corrupted by high energy particles as the satellite passed through the South Atlantic Anomaly (SAA). These SEUs, which now occur roughly once every three days on each detector, have no effect on the science data, but are a potential detector health and safety issue, since corruption of the executing code could cause unpredictable behavior. Although it is not possible to decrease their frequency, their effect has been minimized by developing a procedure by which the instrument flight computer reloads the detector code whenever an SEU is detected. Rarely, about once per month, a potentially more vital part of memory is corrupted,

causing the detector to reboot and turn off the detector high voltage as a safety measure. This currently requires ramping up the high voltage via ground commands, which typically results in a one day loss of data for that detector; this process is now being automated.

## 4. MECHANICAL PERFORMANCE

The FUSE gratings and mirrors are mounted via athermal optical mounts to a carbon fiber structure with an extremely low coefficient of thermal expansion. This system was designed to minimize mechanical variations which might affect the ability to hold the optics stable to several microns over a several meter distance. During the design and construction phase, thermal models were made in order to predict the variations in temperature during an orbit and when changing attitude. Thermistors inside the satellite monitor the temperatures, and the onboard computers control the temperatures to  $\leq 1^\circ\text{C}$  during an orbit. The instrument focus was also adjusted before launch to compensate for the expected changes due to the difference between the ground and on-orbit operating temperature, gravity release, and dimensional changes due to outgassing of water from the structure.

There are two time scales of temperature variations on orbit. The orbital variation is typically  $\sim 1^\circ\text{C}$  internally, but can be as high as  $5^\circ\text{C}$  on external surfaces such as the baffles. In addition, there are long-term temperature variations due to changes in attitude, which lead to different parts of the satellite being illuminated by the sun. These variations can be as large as  $30^\circ\text{C}$ , with a time constant that can be as long as 10 hours, but are more typically 6 hours. This long time constant means that before equilibrium is reached after slewing to a new target, the observation may be completed, and another slew may have taken place.

On orbit we have discovered that thermal changes are inducing higher than expected rotations of both the gratings and mirrors. The rotation of the gratings causes the spectra to move in two dimensions on the detectors in a roughly sinusoidal fashion over the course of an orbit; this degrades the spectral resolution. These motions are as high as  $90\ \mu\text{m}$  ( $0.09\ \text{\AA}$  in wavelength space), depending on the channel. Algorithms have been developed to minimize these shifts during the ground processing of data taken in TTAG mode. These corrections decrease the amplitude of the motion to less than  $0.015\ \text{\AA}$  in wavelength space.

The mirror rotation, which makes it difficult to keep the four channels coaligned, initially resulted in a misalignment large enough for targets to drift out of the LWRS aperture in one or more channels in many instances. We have empirically measured the behavior and limited the frequency of this occurrence to less than  $\sim 10\%$  of observations. An understanding of the drift in more detail is now being obtained as part of a plan to begin making regular observations in the smaller apertures.

A number of workarounds were developed for these problems. These are primarily operational constraints imposed in order to control the moderate thermal variation seen by certain parts of the satellite. Due to satellite power constraints, scattered light, and safety issues, FUSE was designed to operate in the range of  $15^\circ < \beta < 105^\circ$ , where  $\beta$  is the angle between the anti-sun and the satellite optical axis. In order to minimize the mirror motions described above, further constraints have been imposed. Normal operations are now limited to  $30^\circ < \beta < 85^\circ$ . Exceptions are made for specific campaigns, such as a week of observations in the Large Magellanic Cloud at  $\beta \approx 92^\circ$ . During these campaigns, the instrument is allowed to reach thermal equilibrium before a coalignment of the channels is made, and slews are limited to several degrees on the sky between targets in order to minimize drifts of the optics. In addition, regular coalignment operations can be made if channels begin drifting. Characterization is not complete, but it is believed that with the development of thermal models and careful scheduling of observations, this can be improved in the future, allowing reasonable efficiency in the LWRS and MDRS apertures.

## 5. OPTICAL PERFORMANCE

### 5.1. Telescope Performance

The FUSE telescopes provide a complex, non-uniform point spread function at the FPAs. Preflight measurements and analysis<sup>8</sup> of a spare mirror, combined with metrology on the flight mirrors, showed that  $88\pm 5\%$  of the encircled energy is within a  $1.5''$  diameter circle at  $1000\ \text{\AA}$ . In flight, knife edge scans made using the FPAs showed that the telescope PSFs are consistent with these ground measurements. This narrow PSF means that the spectral resolution of point source objects is not limited by the FPA apertures, but rather by the  $\sim 0.3''$  satellite pointing stability and the alignment characteristics described above. The knife edge scans were also used to optimize the mirror to FPA distances, which have been located to  $\pm 50\ \mu\text{m}$ .

## 5.2. Coalignment

The ability to maintain coalignment of the four channels is dependent on knowledge of the thermal and mechanical stability of the system, which affects the rotation of the telescope mirrors. Because of the mechanical instabilities described above, observations in all but the LWRS aperture require multiple peakups per orbit in order to maintain a reasonable throughput. Observations made through the LWRS aperture, where coalignment is much less critical, can typically be maintained for weeks without interruption, with small adjustments of the FPAs and mirrors, as long as pointing angle constraints are followed.

A number of tests have been executed to determine how to most efficiently implement observing in the MDRS and HIRS apertures. Based on data taken for several different targets in the CVZ, the image motions are very repeatable with orbital phase. Using this information allows a determination of when to perform peakups in the MDRS or HIRS aperture as a function of orbital phase, and a prediction of how long we can observe before new peakups are necessary to keep the channels aligned. After more data is obtained, and the shape of this channel motion is well calibrated, we are hopeful that only a single peakup at the beginning of the target's visibility period will be necessary, and then the FPAs can be moved autonomously throughout the orbit in order to keep the channels aligned, thus avoiding the necessity of performing time-consuming peakups throughout the orbit.

## 5.3. Spectrograph Resolution and Instrument Focus

The resolution,  $R = \lambda/\Delta\lambda$ , of the FUSE spectrographs has been determined by measuring the widths of absorption features in the spectra of astrophysical objects. Changes in resolution as a function of wavelength are caused by both the optical design and variations of the intrinsic detector PSF with position. **Figure 3** shows the type of data used to measure resolution; it shows data taken along the line of sight to the white dwarf WD0439+466, which is a hydrogen-rich central star of an old planetary nebula. Since FUSE is limited to observing faint objects, the velocity structure along the line of sight to these objects is often complex, which can significantly broaden the lines. It has been a challenge to find appropriate lines of sight which are known to have narrow lines. At our current focus position, the SiC channels show a resolution of  $\sim 18,000$ , and the LiF channels show  $\sim 23,000$  in the LWRS. Additional adjustments are planned in order to improve these values further. Once optimization is complete, the Science Data Pipeline (see below) will be updated to include the proper algorithms to recover the highest resolution. Most of the earliest FUSE observations were made with the mirrors at their launch position, which yields slightly lower resolution numbers, but are in the 15,000 - 20,000 range. Observations in the smaller apertures, where the positions of the FPAs are important, have begun as the characterization of the thermally-induced mirror motions has been understood in more detail.

In the LWRS aperture, where most observations have been made thus far, the focus of the instrument is determined solely by the position of the mirrors, and the resolution is limited by the telescope PSF, the satellite pointing stability, the mirror and grating stability, and the fact that the LWRS is off axis. The highest possible resolution will require use of the HIRS aperture, but this will likely result in a significant loss of throughput, particularly in the SiC channels.

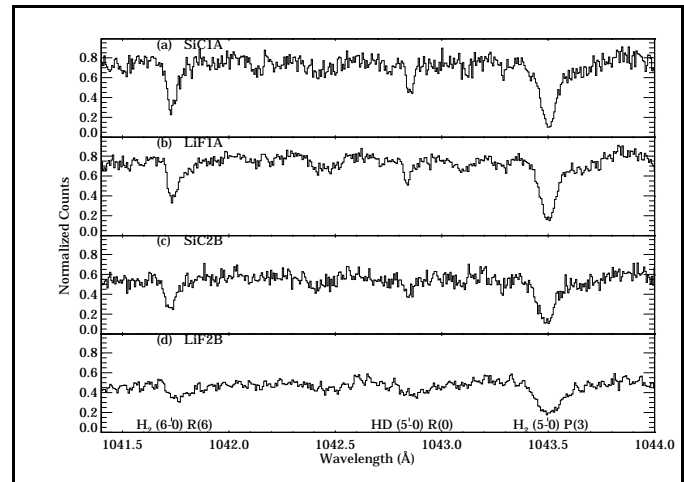


**Figure 3** A spectrum of the line of sight towards WD0439+466 showing the (6-0) R(6) and (5-0) P(3) transitions of  $H_2$ , and the (5-0) R(0) line of HD in all four channels. The variation in resolving power between channels is apparent. The HD line shows a resolving power of up to  $\sim 25,000$ , depending on channel.

## 5.4. Wavelength Calibration

In-flight wavelength calibration is done using astrophysical sources. During spectrograph integration and test, H<sub>2</sub> spectra were used to map the wavelength scale, which is nonlinear because of the variation in size of the of the analog detector pixels with position. High order polynomials were developed to describe this distortion to an accuracy of better than one spectrograph resolution element, which is expected to remain stable, aside from the expected stretches and shifts caused by variations in detector temperature. A combination of downward looking airglow and astronomical sources is being used to tie the ground-based solution to the in flight data.

## 5.5. Scattered Light

Scattered light is known to be present at several levels. A vertical “stripe” of enhanced counts is present on one detector segment; its intensity varies with the Lyman-β airglow, so it is thought to be caused by light entering the spectrograph from a stray light path. In addition, the overall background rate is seen to vary between day and night. Both of these effects are at a level of a few percent, so they have an effect on the data for only the lowest flux targets, and then typically only near the bottom of saturated lines<sup>1</sup>.

## 6. SENSITIVITY

The current estimate of the effective area, based primarily on observations of hot hydrogen-rich white dwarf stars, is shown in **Figure 4** for each of the channels as a function of wavelength. Errors are estimated to be 10%, and will decrease as more measurements are made. As part of our regular calibration program, we return to these calibration targets roughly once per month in order to monitor the expected decrease in effective area with time. Early indications are that this drop is less than the budgeted 20% per year.

The high throughput of the LiF channels below ~1000 Å is a result of the great lengths to which the FUSE project went in order to minimize exposure of these optics to air with a relative humidity above ~50%. As the LiF coating absorbs water, the short wavelength cutoff moves to longer wavelengths<sup>9</sup>. Maintaining high sensitivity at OVI λλ1036, 1038 Å, in particular, is important to the scientific goals of the FUSE mission. The mirrors and gratings were exposed to room air with a humidity > 30% for a total of only five days during all instrument and subsystem testing.

Similar efforts were made to minimize particulate, and molecular contamination in the instrument. An additional precaution taken in order to keep the reflectivities high was limiting pointing to only the continuous viewing zone (CVZ) for the first part of the mission. During a typical observation, a target is occulted by the earth every orbit. Since the satellite remains pointed at the object (using its onboard gyros rather than the FES), the bright earth illuminates the mirrors each time this happens. Ultraviolet light from the earth can lead to a polymerization of contaminants on the optics. For this reason, potential molecular contaminants were limited in the construction of the satellite – particularly in the optical cavity which contains the mirrors and gratings. Restricting early pointings to the CVZ allowed as much of the contamination as possible to outgas in order to limit these effects. In addition, the grating and mirror surfaces are being kept several degrees warmer than the surrounding surfaces in order to minimize condensation of contaminants.

To further limit on-orbit degradation of the mirror reflectivities, a ram avoidance angle of 20° has been implemented as an operations constraint, in particular to avoid atomic oxygen directly striking the SiC channel telescope mirrors. Atomic oxygen has been implicated in the loss of reflectivity of SiC optics on numerous other space missions<sup>10,11</sup>.

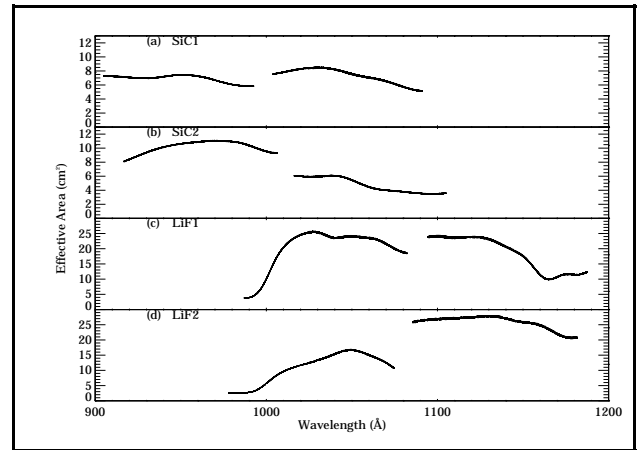


**Figure 4** Estimated effective area of the four channels of the FUSE instrument, based on measurements of white dwarfs and model spectra. Due to variations in coating reflectivity, grating efficiency, and detector sensitivity, there is a substantial variation between channels. Note that the scales are different for the SiC and LiF channels.

An optical anomaly which affects the flux calibration has been discovered in the data. It consists of a roughly horizontal band with a deficit of counts, and seems to appear in nearly all spectra. It is visible on all four channels, most prominently at wavelengths where the astigmatic height is the largest. Its location in wavelength space changes with time, so it seems to be an optical effect, most likely due to the gratings. Since it is not stable with time, it makes flux calibration uncertain in the regions where it is most prominent. It is not understood at this time.

## 7. OPERATIONS

### 7.1. Mission Operations

Mission operations is run from the FUSE Satellite Control Center (SCC) at the Johns Hopkins University, where science and mission operations are co-located. Planning and scheduling of observations, generation of command loads, communication with the satellite through an autonomous ground station, receipt and processing of science and engineering data, monitoring of the health and safety of the satellite and instrument, computation of the FUSE orbital elements, off-line analysis of science and engineering data, and maintenance of flight software all occur at this facility.

Communications with FUSE is primarily through a dedicated ground station antenna located at the University of Puerto Rico in Mayaguez (UPRM). When FUSE passes within range of the ground station, communication is possible for only about 10 minutes of the 100 minute orbit, on average. Furthermore, due to the  $25^\circ$  inclination of the orbital plane, there is a  $\sim 12$  hour period every day when there is no communication possible from UPRM. Consequently, a high degree of autonomy has been built into the satellite to allow unaided target and guide star acquisitions, instrument alignment, and health and safety checks of the instrument by flight software. Observations proceed autonomously with no intervention from the ground.

Science data are transmitted to the ground station at 1 megabit/sec and are stored locally on disk at the ground station. The data are then transmitted to the SCC via an ISDN line after the ground station contact is over. Level zero processing in the SCC removes the downlink packet structure from the data, which is then sent through the OPUS pipeline<sup>12</sup> and the CALFUSE pipeline, where the spectra are corrected for instrumental effects, turned in to one-dimensional spectra, and calibrated. After calibration, the data are archived by the Multimission Archive at the Space Telescope Science Institute (MAST).

Overall observing efficiency is limited by the low earth orbit, which results in most targets being occulted for part of every orbit. In addition, observations cannot be made during SAA passages, and slewing and peakups add overhead. The mirror motions described in section 4 also decrease the efficiency of observations in the MDRS and HIRS slits. Despite these constraints, the on-orbit efficiency is close to that predicted before launch, and slowly increasing as the number of calibration observations and other special tests decreases with time.

### 7.2. Event Bursts

An unexplained feature observed in the data is the intermittent increase in the count rate, from an as yet undetermined source. The pulse height distributions of these "event bursts" are consistent with the distributions exhibited by photons, so they are apparently due to light rather than particles or some other source internal to the detector. The source of these photons is unknown, however.

These bursts have durations that range from a few to several hundred seconds, and maximum intensities that are typically 20,000 per second. Their occurrence is uncorrelated with orbital location, ram vector, or other orbital phenomena have been unsuccessful, although they occur primarily in orbital morning, with many occurring near noon. Early in the mission, while the satellite was pointed in the continuous viewing zone in order to avoid observing the bright earth, they occurred on nearly every orbit. The frequency has dropped significantly since that time, but it is unclear if that is an effect of changes in pointing geometry due to constraints provided by the mirror and grating motions, or some other effect, such as a lower pressure in the spectrograph cavity.

Since the bursts are isolated in time, rarely occurring more than once per orbit, they can easily be screened from time tag data during ground processing without a significant loss of observing efficiency; a pipeline module to automatically remove these times from the data is currently under development. It is not possible to remove them from spectral image data, but since these observations typically have much higher count rates, the bursts provide much less contamination.

## 8. SUMMARY

The *FUSE* satellite, in its first eight months on orbit, has generally been performing well. High quality data is being obtained routinely (see, for example, **Figure 5**), and workarounds are being developed for the anomalies that have been discovered since launch. The performance of the instrument exceeds the level necessary to perform first-class science, for both the Principal Investigator team projects and Guest Investigator programs. All onboard systems are performing as designed or better; no component failures have occurred. Now that routine operations have been underway for some time, work on

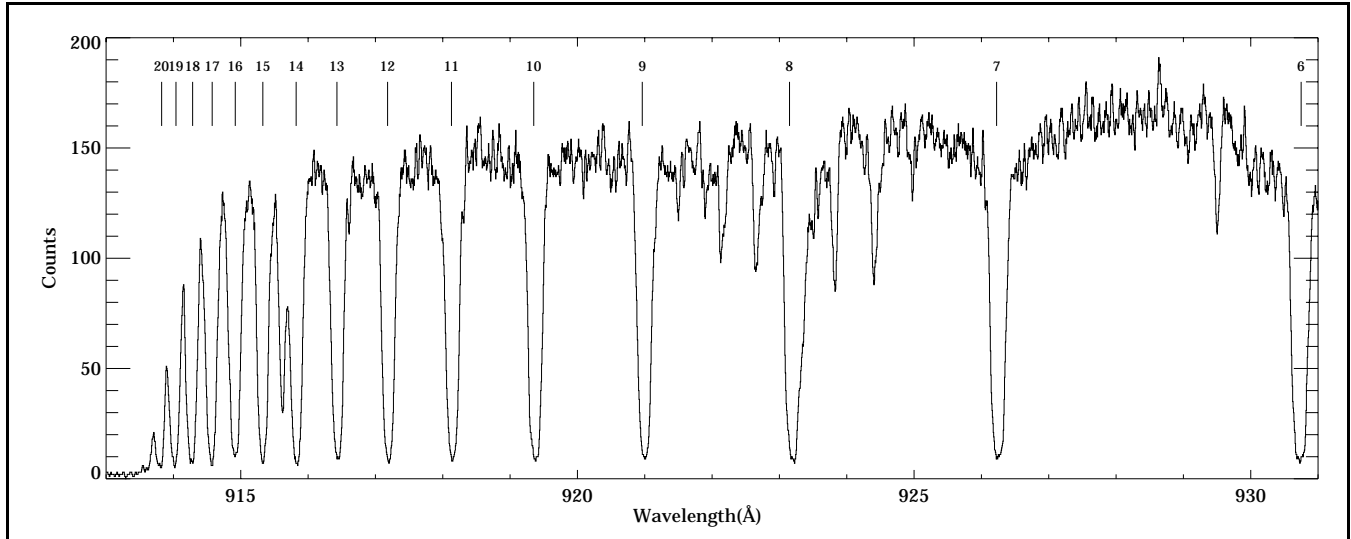


**Figure 5** Broad photospheric ( $L_6$  and  $L_7$ ) and narrow interstellar ( $L_6$  to  $L_{20}$ ) Lyman series lines measured with *FUSE*, in the photosphere and along the line of sight to the hydrogen-rich white dwarf star WD2211-495.

modifications to procedures and algorithms in order to maximize the scientific return of the observatory, and refine its characterization have begun.

Additional information on the *FUSE* mission can be found at <http://fuse.pha.jhu.edu>.

## ACKNOWLEDGMENTS

We gratefully acknowledge the contributions of the many people who have contributed to the success of the *FUSE* mission. This work is based on data obtained by the NASA-CNES-CSA *FUSE* mission operated by the Johns Hopkins University. Financial support to U. S. participants has been provided by NASA contract NAS5-32985.

## REFERENCES

1. H. W. Moos et al., "Overview of the Far Ultraviolet Spectroscopic Explorer Mission," *ApJ* 2000, submitted.
2. S. D. Friedman, S. J. Conard, R. H. Barkhouser, K. R. Brownsberger, A. N. Cha, A. W. Fullerton, J. W. Kruk, H. W. Moos, E. M. Murphy, R. J. Ohl, D. J. Sahnou, and H. A. Weaver, "Pre-launch optical tests and performance estimates of the Far Ultraviolet Spectroscopic Explorer satellite," *Proc. SPIE* **3765**, 460-469, 1999.
3. D. J. Sahnou, S. D. Friedman, W. R. Oegerle, H. W. Moos, J. C. Green, and O. H. W. Siegmund, "Design and predicted performance of the Far Ultraviolet Spectroscopic Explorer (*FUSE*)," *Proc. SPIE* **2807**, pp. 2-10, 1996.
4. A. N. Cha, D. J. Sahnou and H. W. Moos, "Processing and interpretation of pre-flight *FUSE* spectra," *Proc SPIE*, **3765**, 495-505, 1999.

5. O. H. W. Siegmund, M. Gummin, G. Gaines, G. Naletto, J. Stock, R. Raffanti, J. Hull, R. Abiad, T. Rodriguez-Bell, T. Magoncelli, P. Jelinsky, W. Donakowski, and K. Kromer, "Performance of the double delay line microchannel plate detectors for the Far Ultraviolet Spectroscopic Explorer," *Proc. SPIE* **3114**, pp. 283-294, 1997.
6. A. S. Tremsin, O. H. W. Siegmund, M. A. Gummin, P. N. Jelinsky, and J. M. Stock, "Electronic and optical moiré interference with microchannel plates: artifacts and benefits," *Appl. Opt.* **38**, 2240-2248, 1999.
7. O. H. W. Siegmund, J. Vallergera and B. Wargelin, "Background events in microchannel plates," *IEEE Trans. Nucl. Sci.*, **35**, 524-528, 1988.
8. R. G. Ohl, T. T. Saha, S. D. Friedman, R. H. Barkhouser and H. W. Moos, "Imaging performance of telescope mirrors for far-ultraviolet astronomy," *Appl. Opt.*, 2000, in press.
9. C. M. Oliveira, K. Retherford, S. J. Conard, R. H. Barkhouser, and S. D. Friedman, "Aging studies of LiF coated optics for use in the far ultraviolet," *Proc. SPIE*, **3765**, 52-60, 1999.
10. H. Herzig, A. R. Toft and C. M. Fleetwood, Jr. "Long-duration orbital effects on optical coating materials," *Appl. Opt.* **32**, 1798-1804, 1993.
11. J. F. Seely, G. E. Holland, W. R. Hunter, R. P. McCoy, K. F. Dymond and M. Corson, "Effect of oxygen bombardment on the reflectance of silicon carbide mirrors in the extreme ultraviolet region," *Appl. Opt.* **32**, 1805-1810, 1993.
12. J. F. Rose, C. Heller-Bowyer, M. A. Rose, M. Swam, W. Miller, G. A. Kriss and W. R. Oegerle, "OPUS: The FUSE Science Data Pipeline," *Proc. SPIE* **3349**, pp. 410-420, 1998.